https://doi.org/10.5194/cp-2020-87
Preprint. Discussion started: 20 July 2020

Climate of the Past Discussions

Reconstructing past hydrology of eastern Canadian boreal catchments using clastic varved sediments and hydro-climatic modeling: 160 years of fluvial inflows

Antoine Gagnon-Poiré[1-5], Pierre Brigode[2], Pierre Francus[1-3-5], David Fortin[1-6], Patrick Lajeunesse[4-5], Hugues Dorion[4] and Annie-Pier Trottier[4-5]

[1] *Institut national de la recherche scientifique, Centre Eau Terre Environnement*
[2] *Université Côte d'Azur, CNRS, OCA, IRD, Géoazur, Nice, France.*
[3] *Chaire de recherche du Canada en Sédimentologie environnementale and GEOTOP, Geochemistry and Geodynamics Research Center, Montréal, QC, Canada.*
[4] *Département de géographie, Université Laval, Québec, QC, Canada.*
[5] *Centre d'études nordiques, Québec, QC, Canada.*
[6] *Department of Geography and Planning, University of Saskatchewan, Saskatoon, SK, Canada*

Corresponding author: Antoine Gagnon-Poiré (Antoine.Gagnon-Poire@ete.inrs.ca)

https://doi.org/10.5194/cp-2020-87
Preprint. Discussion started: 20 July 2020

Abstract

Analysis of short sediment cores collected in Grand Lake, Labrador, revealed that this lake is an excellent candidate for the preservation of laminated sediments record. The great depth of Grand Lake, the availability of fine sediments along its tributaries, and its important seasonal river inflow have favored the formation of a 160 years-long clastic varved sequence. Each varve represents one hydrological year. Varve formation is mainly related to spring discharge conditions with minor contributions from summer and autumn rainfall events. The statistically significant relation between varve parameters and the Naskaupi river discharge observations provided the opportunity to develop local hydrological reconstructions beyond the instrumental period. Mean detrital layer thickness and the grain-size (99th percentile) series extracted from each varve yields the strongest correlations with instrumental data (r = 0.69 and 0.76) and have been used to reconstruct Naskaupi River mean and maximum annual discharges, respectively, over the 1856-2016 period. The reconstructed Q-mean series suggest that high Q-mean years occurred during the 1925-1960 period and a slight decrease in Q-mean take place during the second half of the 20th century. Independent reconstructions based on rainfall-runoff modeling of the watershed from historical reanalysis of global geopotential height fields display a significant correlation with the reconstructed Naskaupi River discharge based on varve physical parameters. The Grand Lake varved sequence contains a regional hydroclimatic signal as suggested by the statistically significant relation between mean detrital layer thickness series and the observed Labrador region Q-mean series extracted from five watersheds of different size and location.

1. Introduction

Climate changes caused by rising concentrations of greenhouse gases can alter hydro-climatic conditions on inter- and intra-regional scales (Linderholm et al., 2018; Ljungqvist et al., 2016; Stocker et al., 2013). Hydropower, which is considered as a key renewable energy source to mitigate global warming, has strong sensitivity to changes in hydrological regime especially in vulnerable northern regions (Cherry et al., 2017). Therefore, a clear understanding of the regional impacts that recent climate change combined with natural climate variability can have on river discharge and hydroelectric production is needed.

https://doi.org/10.5194/cp-2020-87
Preprint. Discussion started: 20 July 2020

However, the lack of instrumental records and the uncertainty related to hydroclimate variability projections (Collins et al., 2013) are obstacles to sustainable management of these water resources.

The Labrador region in eastern Canada is a critical area for hydropower generation, hosting the Churchill River hydroelectric project, one of the largest hydropower systems in the world. Average annual streamflow has been varying in eastern Canada during the last sixty years, with higher river discharges from 1961 to 1979 and 1990 to 2007, and lower discharges from 1980 to 1989 (Mortsch et al., 2015; Déry et al., 2009; Jandhyala et al., 2009; Sveinsson et al., 2008; Zhang et al. 2001). These changes in streamflow represent a significant economic challenge for the long-term management of hydropower generation. The few decades of available instrumental observations (<60 years) and their low spatial coverage are not sufficient to allow a robust analysis of multi-decadal hydrological variability.

The study of multi-decadal hydrological variability requires long instrumental records (>100 years), but such long-time series are non-existent for the Labrador region. Recently, rainfall-runoff modeling approaches have been used to expand instrumental streamflow datasets, using long-term climatic reanalysis as inputs. Rainfall-runoff modeling was used by Brigode et al. (2016) to reconstructed daily streamflow series over the 1881–2011 period in northern Québec. Nevertheless, this type of methods suffers from the limited observations in order to evaluate and validate the reconstructed hydro-climatic temporal series. The deficiency of observations led to the exploration of various natural archives for reconstructing past hydro-climatic conditions. Long hydro-climatic series based on natural proxies in the study region are rare and limited to tree-ring (Dinnis et al., 2019; Boucher et al., 2017; Begin et al., 2015; Naulier et al., 2015; Naulier et al., 2014; Nicault et al., 2014; Boucher et al., 2011; Begin et al., 2007; D'Arrigo et al., 2003) and pollen datasets (Viau et al., 2009). In this perspective, clastic varves formed and preserved in river-fed lakes have the potential to produce long paleohydrological series. Clastic varves can provide, in favourable settings, annually to seasonally resolved information about downstream sediment transport from the catchment area the into lake basin depending on regional

https://doi.org/10.5194/cp-2020-87
Preprint. Discussion started: 20 July 2020

hydro-climatic conditions (Lamoureux, 2000; Lamoureux et al., 2006; Tomkins et al., 2010; Cuven et al., 2011; Kaufman et al., 2011; Schillereff et al., 2014; Amann et la., 2015; Heideman et al., 2015; Zolitschka et al., 2015; Saarni et al., 2016; Czymzik et al., 2018).

Preliminary analysis of short sediment cores collected in Grand Lake, central Labrador, revealed that this lake is an excellent candidate for the preservation of recent fluvial clastic laminated sediments record (Zolitschka et al., 2015). The objectives of this paper are to: (1) Confirm the annual character of the laminations record; (2) Establish the relation between the physical parameters of laminations and local hydro-climatic conditions to examine the potential proxy for hydrological reconstructions; (3) Reconstruct the hydrology of the last 160 years and compare its similarities and differences with Brigode et al. (2016) rainfall-runoff modelling over the 1880-2011 period; and (4) Determine if there is a Labrador regional streamflow signal recorded in Grand Lake laminated sediments.

2. Regional setting

Grand Lake is a 245-m-deep (Trottier et al., 2020) elongated (60-km-long) fjord-lake located in a valley connected to the Lake Melville graben in central Labrador (53°41'25.58"N, 60°32'6.53"O, ~15 m above sea level) (Fig. 1). The region is part of the Grenville structural province and is dominated by Precambrian granite, gneiss and acidic intrusive rocks. Grand Lake watershed deglaciation began after ~8.2 cal ka BP (Trottier et al., 2020). During deglaciation, marine limit reached an elevation of 120-150 m above modern sea level and invaded further upstream in the modern fluvial valleys that are connected to the lake (Fizthugh, 1973). This former glaciomarine/marine sedimentary fjord basin has been glacio-isostatically uplifted and isolated by a morainic sill to become a deep fjord-lake (Trottier et al., 2020). The regional geomorphology is characterized by glacially sculpted bedrock exposures, glacial deposits consisting of till plateaus of various elevations, glacial lineations, drumlins, kames, eskers and raised beaches (Fulton 1992). Podzolic soils dominate, with inclusions of brunisols and wetlands.

https://doi.org/10.5194/cp-2020-87
Preprint. Discussion started: 20 July 2020

Climate of the Past
Discussions

Grand Lake is located in the High Boreal Forest ecoregion, one of the most temperate climates in Labrador (Riley et al., 2013). This region is influenced by temperate continental (westerly and southwesterly winds) and maritime (Labrador Current) conditions with cool humid summers (~8.5 °C) and cold winters (~-13 °C). The Grand Lake watershed extends upstream over the low subarctic Nipishish-Goose ecoregion, a broad bedrock plateau (<700 m.a.s.l.) located on the west flank of the Lake Melville lowlands. With cooler summers and and longer cold winters, this area is slightly influenced by the Labrador Sea. Mean annual precipitation in the study region ranges from 800 mm to 1 000 mm, with 400 cm to 500 cm of snowfall. The regional hydrological regime typically exhibits winter low flow and spring freshet, followed by summer flow recession (Fig. 2). Snowmelt in Grand Lake region takes place from April to June (AMJ).

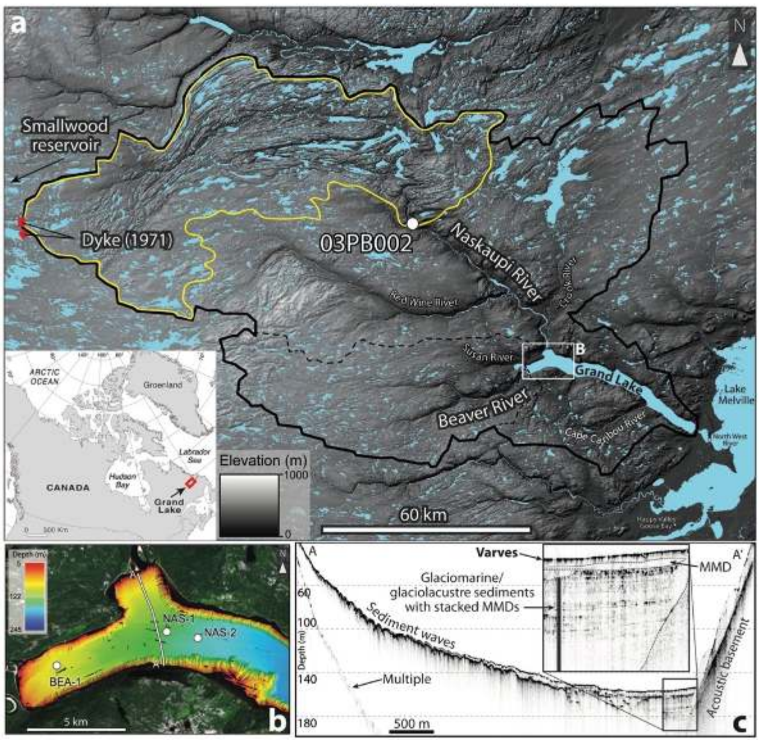

Figure 1. (A) Location of Grand Lake watershed (black line) and its principal tributaries. The Naskaupi River hydrometric station (03PB002: white dot) covering an area of 4480 km^2 (yellow line). Location of the dykes constructed in 1971 to divert water from the Naskaupi River to the Smallwood reservoir hydroelectric system are also shown by the red bars. (B) High-resolution swath bathymetry (1-m resolution) of Grand Lake (Trottier et al., 2020) coupled with a Landsat image (USGS) and core locations. The white line indicates the location of a typical 3.5 kHz subbottom profile (C) of the Naskaupi River delta (A-A').

https://doi.org/10.5194/cp-2020-87
Preprint. Discussion started: 20 July 2020

The main tributary of Grand Lake is the Naskaupi River located at the lake head (Fig. 1). The downstream part of the Naskaupi River is fed by the Red Wine and the Crook rivers. The Beaver River is the secondary tributary of Grand Lake. Naskaupi and Beaver rivers structural valleys that connect to the Grand Lake Basin have a well-developed fluvial plain and a generally sinuous course that remobilize former deltaic systems and terraces composed of glaciomarine, marine, fluvio-glacial, lacustrine and modern fluvial deposits. River terraces show mass movement scarps and are affected by gully and eolian activity. Grand Lake flows into a small tidal lake (Little Lake) and subsequently towards Lake Melville. On 28 April 1971, by closing a system of dykes, the headwaters of Naskaupi River watershed (Lake Michikamau) were diverted into the Churchill River hydropower development (Fig. 1a). This diversion has reduced the drainage area of the Naskaupi river from 23 310 km^2 to 12 691 km^2 (Anderson, 1985).

Hydroacoustic data were collected in Grand Lake in 2016 (Trottier et al., 2020). The swath bathymetric imagery and 3.5 kHz subbottom profile show that the prodelta slopes present well-defined sediment waves at the Naskaupi River mouth (Trottier et al., 2020; Fig. 1b). The upper acoustic unit is composed of a high amplitude acoustic surface changing into low amplitude acoustic parallel reflections (Fig. 1c), a type of acoustic facies which can be associated with successive sedimentary layers of contrasting particle sizes (Gilbert and Desloges, 2012).

https://doi.org/10.5194/cp-2020-87
Preprint. Discussion started: 20 July 2020

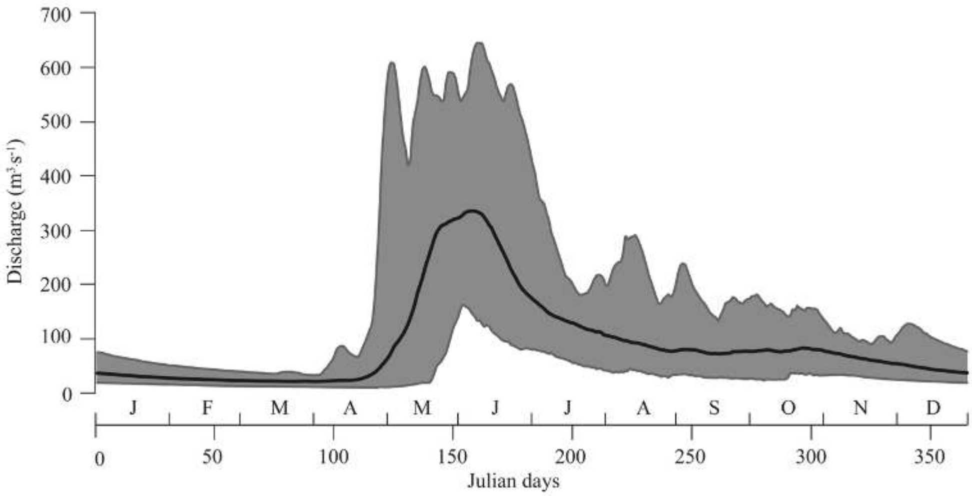

Figure 2. Observed mean daily discharges of the Naskaupi River (hydrometric station 03PB002) for the 1978-2012 period (black line). The gray zone represents the minimum and maximum observed discharges.

3. Methods

3.1 Sediment coring and processing

Four short sediment cores (BEA-1, NAS-1A, NAS-1B and NAS-2) were collected using a UWITEC percussion corer in March 2017. These cores were collected in undisturbed area according to the swath bathymetry and subbottom profiling data (Trottier et al., 2020) in the axis of the Beaver (BEA-1) and Naskaupi (NAS-1, NAS-2) river mouth at a depth of 93, 146 and 176 m respectively. Site NAS-1 is located at the distal frontal slope of the Naskaupi River delta slope; site NAS-2 is located away from the delta, at the beginning of the deep lake basin. Efforts were made to retrieve the cores without disturbing the sediment water interface. Duplicate cores have been retrieved at each site to maximize the sediment recovery. The cores were scanned using a Siemens SOMATOM Definition AS+ 128 medical CT-Scanner at the multidisciplinary laboratory of CT-scan for non-medical use of the Institut National de la Recherche Scientifique - Eau Terre Environnement (INRS-ETE). The CT-scan images allowed the identification of sedimentary structures (i.e., laminated facies, perturbation and hiatus). Expressed as CT-numbers or Hounsfield units (HU), X-Ray attenuation is function of density and the effective atomic number, and hence sensitive to contrasts in mineralogy, grain size and sediment porosity (St-Onge et al., 2007). CT-

https://doi.org/10.5194/cp-2020-87
Preprint. Discussion started: 20 July 2020

numbers were extracted at a resolution of 0.06 cm using the ImageJ software 2.0.0 (imagej.net). The cores were then opened, described and photographed with a high-resolution line-scan camera mounted on an ITRAX core scanner (Cox Analytical Systems, Sweden) (RGB color images; 50 µm-pixel size). Geochemical non-destructive X-Ray Fluorescence (XRF) analysis was performed on the core half (30 kV and 30 mA) at the INRS-ETE. XRF elements profiles were used to visualize varves and their sub-layer boundaries, micro-facies and estimate particle-size variability in sediment cores (Kylander et al., 2011; Cuven et al., 2010; Croudace et al., 2006). The element abundances are expressed in counts per second (cps). Continuous XRF measurements were also carried out on overlapping impregnated sediment blocks in order to superpose element abundance profiles on thin-sections.

3.2 Chronology and thickness measurement

Surface sediments from cores BEA-1 and NAS-1A were dated with ^{137}Cs method (Appleby and Oldfield 1978) using a high-resolution germanium diode gamma detector and multichannel analyzer gamma counter. A sampling interval of 2 cm to ±0.5 cm was used in order to sample each lamination for the 1961-1965 period. ^{137}Cs activity was used to identify sediment deposited during 1963-1964 peak of nuclear tests and validate the annual character of the layers. In order to establish a chronology for each core, detailed laminations counts were executed repeatedly on CT-scan images and high-resolution photographs using ImageJ 2.0.0 and Adobe Illustrator CC softwares. As all of the core surface has been well preserved, the first complete lamination below the sediment surface was considered to represent the topmost year (i.e., 2016 CE). Chronology on each sediment core was confirmed by cross-correlation between visual thick marker beds (A to P; Fig. 4).

Thin-sections of sediments were sampled from core BEA-1 and NAS-1A, NAS-1B and NAS-2 (see Fig. 4 for thin-section location) following Francus and Asikainen (2001) and Lamoureux (1994). Digital images of the thin-sections were obtained using a transparency flatbed scanner at 2400 dpi resolution (1 pixel = 10.6 µm) in plain light and were used to characterize lamination sub-layers. Lamination counts and thickness measurements using a thin-section image analysis software developed at INRS-ETE (Francus and Nobert 2007)

https://doi.org/10.5194/cp-2020-87
Preprint. Discussion started: 20 July 2020

Climate of the Past
Discussions

were performed to duplicate and validate previous chronologies established on CT-Scan images and high-resolution photographs. Total Varve Thickness (TVT) and Detrital Layer Thickness (DLT) of each year of sedimentation were measured from images of thin-sections. Lamination counts made on CT-scan images, high-resolution photographs and thin-sections are identical while TVT measurements show negligible difference ($R^2 = 0.96$; $p < 0.01$). The thickness measurements made from CT-scan images and high-resolution photographs have been used to prolong the TVT series of core NAS-2 from 1968 back to 1856. Continuous varve thickness measurements allowed the establishment of high-resolution age-depth models for the three sites.

3.3 Image and particle-size analysis

Using a custom-made image analysis software (Francus and Nobert 2007), regions of interest (ROIs) were selected on the thin-section images. The software then automatically yielded SEM images of the ROIs using a Zeiss Evo 50 scanning electron microscope (SEM) in backscattered electron (BSE) mode. Eight-bit gray-scale BSE images with a resolution of 1024 x 768 pixels were obtained with an accelerating voltage of 20 kV, a tilt angle of 6.1 and an 8.5 mm working distance with a pixel size of 1 µm. BSE images were processed to obtain black and white images where clastic grains (>3.5 µm) and clay matrix appeared black and white respectively (Francus, 1998).

Each sedimentary particle (an average of 2 225 particles per image) was measured according to the methodology used by Lapointe et al. (2012), Francus et al. (2002) and Francus and Karabanov (2000) in order to calculate particle-size distribution on each ROI image. Due to the important thickness of the laminations, results from several ROI images were merged to obtain measurements for each year of sedimentation, with an average of 4 images per lamination. Only clastic facies related to spring and summer discharges were used for particle-size analysis in order to exclude coarse debris observed in the early spring sub-layer (see Fig. 5 for details). Particle size indice (PSI) for each lamination (percentile 99 % ($P99D_0$)) (Francus, 1998), was analyzed from thin-sections for the last 160 years (1856-2016) for core BEA-1 and NAS-1, and for 47 years (1969-2016) for core NAS-2, from 795, 717 and 132 BSE images respectively (Fig. 4).

https://doi.org/10.5194/cp-2020-87
Preprint. Discussion started: 20 July 2020

3.4 Hydro-climatic variables used

Hydrological variables (Tab.1) were calculated from the time series of daily discharges recorded by the Naskaupi river hydrometric station over the 1978-2011 period (missing data from the years 1996, 1997 and 1998).

Table 1. Hydro-climatic variables used in this paper

Hydrological variable	Unit	Description
Q-max	m^3/s	Annual maximum of daily discharges
Q-mean	m^3/s	Mean annual discharge
Q-max-JJ	Julian days	Julian day at which the discharge reaches its maximum annual value
Rise-Time	Days	Number of days between the minimum winter flow and the maximum spring flow
Nb-Days-SupQ80	Days	Number of days with discharge greater than the 80^{th} daily percentile
E-Qnival	mm	Nival runoff (April, May, June, July)
Snow-Win	mm	Winter snowfall (September to May)
Ptot_Annual	mm	Winter Snowfall + Summer rainfall
Ptot-Summ	mm	Summer rainfall (March to October)
Temp-Spring	°C	Average spring temperature (April, May, June)

The Naskaupi River hydrological variables have been compared with four other hydrometric station data available around the study region (Fig. 3a). These series are devoid of anthropogenic perturbations. These four streamflow series (Tab. 2) show strong positive correlations with Naskaupi River discharge. Q-mean series from the five stations (Fig. 3a, Tab. 2;) have been normalized for the common 1979–2011 period and averaged, to produce a Labrador region mean annual discharge series. This allows to extend instrumental data series until 1969 to 2011 and fill in data for the missing years. The Labrador hydrometric station data used in this study come from a Government of Canada website (https://wateroffice.ec.gc.ca 05/2018).

Table 2. Description of hydrometric stations used in this study

Hydrometric station	ID	Area (km2)	Location (N,W)	Recording period (A.D.)
Ugjoktok River	03NF001	7570	55° 14' 02", 61° 18' 06"	1979-2016
Naskaupi River	03PB002	4480	54° 07' 54", 61° 25' 36"	1978-2011
Minipi River	03OE003	2330	52° 36' 45", 61° 11' 07"	1979-2014
Little Mecatina River	02XA003	4540	52° 13' 47", 61° 19' 01"	1978-2016
Eagle River	03QC001	10 900	53° 32' 03", 57° 29' 37"	1966-2016

https://doi.org/10.5194/cp-2020-87
Preprint. Discussion started: 20 July 2020

3.5 Linear regression of varve properties on hydrological variables

A simple linear regression model was used to fit the normalized mean TVT, DLT and $P99D_0$ series with local (1978-2011) and regional (1969–2016) instrumental series and reconstructed hydrological variables (Q-mean, Q-max) back to 1856. Models calibration was performed using a twofold cross-validation technique over the instrumental period. Root mean squared errors (RMSE) and adjusted coefficient of determination (adj R^2) were calculated for calibration periods, while average reduction of error (RE) and average coefficient of efficiency (CE) were calculated to evaluate reconstruction skills (Briffa et al. 1988, Cook et al., 1999). Statistical analysis was realized using the R-project environment (R Core Team, 2019, http://www.r-project.org/).

3.6 Hydro-climatic reconstruction based on rainfall-runoff modeling

The applied reconstruction method is based on rainfall-runoff modeling. Firstly, it aims at producing, for each studied catchment, daily climatic time series using a historical reanalysis of global geopotential height fields extracted over the studied region for a given time period (here 1880-2011). Secondly, the produced climatic series are used as inputs to a rainfall–runoff model previously calibrated on each studied catchment in order to obtain daily streamflow time series. The reconstruction method, fully described in Brigode et al. (2016) and recently applied over southeastern Canada catchments in Dinis et al. (2019), is summarized in the following paragraphs.

For each studied catchment, the available observed hydro-climatic series have been aggregated at the catchment scale. Table 2 lists the recording periods of each hydrometric stations. Climatic series (daily air temperature and precipitation) have been extracted from the CANOPEX dataset (Arsenault et al., 2016), built using Environment Canada weather stations and Thiessen polygons to calculate climatic series at the catchment scale. Daily air temperature series have been used for calculating daily potential evapotranspiration at the catchment scale, thanks to the Oudin et al. (2005) formula, designed for rainfall-runoff modelling.

https://doi.org/10.5194/cp-2020-87
Preprint. Discussion started: 20 July 2020

Climate of the Past
Discussions
Open Access
EGU

These daily series have been used for calibrating the GR4J rainfall-runoff model (Perrin et al., 2003) and its snow accumulation and melting module, CemaNeige (Valéry et al., 2014a), using the airGR package (Coron et al., 2017). This combination of GR4J and CemaNeige (hereafter denoted CemaNeigeGR4J) has been recently applied over eastern Canada catchments and showed good modelling performances (e.g., Seiller et al., 2012; Valéry et al., 2014b, Brigode et al., 2016). CemaNeigeGR4J has been calibrated on the recorded period of each catchment using the Kling and Gupta efficiency criterion (Gupta et al., 2009) as objective function.

Then, the observed climatic series have been resampled over the 1880-2011 period, based on both season and similarity of geopotential height fields (Kuentz et al., 2015). The resampling is performed by calculating Teweles and Wobus (1954) distances between four geopotential height fields: (i) 1000 hPa at 0 h, (ii) 1000 hPa at 24 h, (iii) 500 hPa at 0 h, and (iv) 500 hPa at 24 h. The NOAA 20th Century Reanalysis ensemble (Compo et al., 2011, hereafter denoted 20CR) has been used as a source of geopotential height fields (Fig. 3b).

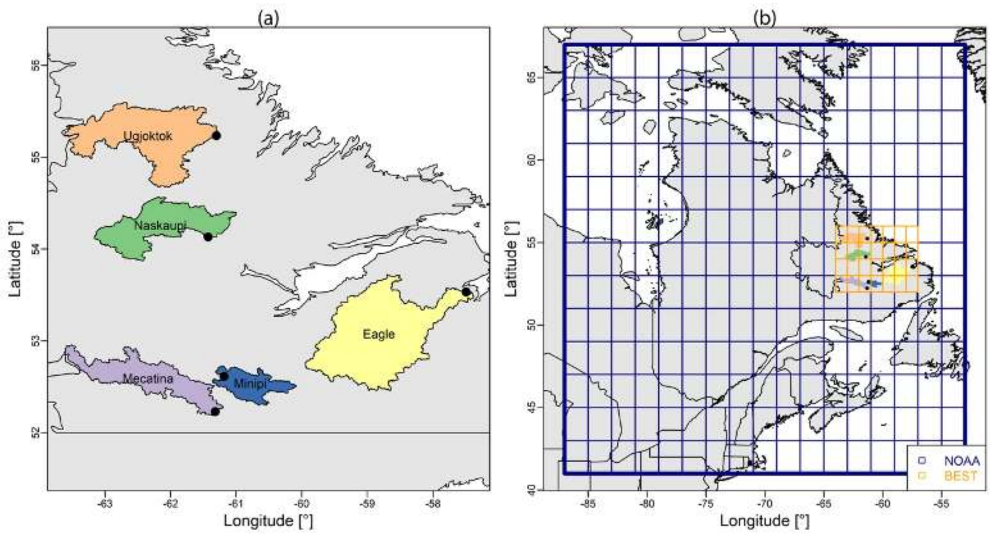

Figure 3. (a) Dataset used for the hydro-climatic reconstruction based on rainfall-runoff modeling: the extension of the 20CR grid used is shown in blue, while the BEST grid used is highlighted in orange. (b) Spatial distribution of hydrometric stations used in this study (black dots) and their catchment area.

https://doi.org/10.5194/cp-2020-87
Preprint. Discussion started: 20 July 2020

Climate of the Past
Discussions

As in Brigode et al. (2016), the resampled series of air temperature have been corrected at the catchment scale thanks to a regression model calibrated with the Berkeley Earth Surface Temperature analysis (Rohde et al., 2013, hereafter denoted BEST). BEST is a gridded air temperature product starting in 1880 at the daily timestep (Fig. 3b).

Finally, the daily climatic series are, for each studied catchment, used as inputs to the CemaNeigeGR4J model in order to obtain daily streamflow time series on the same 1880-2011 period. Thus, the outputs of the hydro-climatic reconstruction are, for each catchment, an ensemble of daily meteorological series (air temperature, potential evapotranspiration and precipitation) and an ensemble of daily streamflow series.

4. Results

4.1 Lamination characterization

Sediment retrieved at the head of Grand Lake (Fig. 4), consist of dark grayish to dark yellowish brown (Munsell color: 10YR-4/2 to 10YR-4/4) laminated minerogenic material, interpreted as clastic lamination of fluvial origin. Lamination structure can be divided in 3 seasonal sub-layers (Fig. 5) based on their stratigraphic position and microfacies. Annual sedimentation starts with a sub-layer composed of silt and clay sediment matrix which sometimes contains ice-rafted debris (IRD) (µm to cm scale) interpreted as an Early Spring Layer (ESL). The major varve component is a spring and summer/autumn Detrital Layer (DL). The thick basal part of the DL is mostly poorly sorted, graded and composed of coarse minerogenic grains comprising fine sand and silts (< 150 µm) with some redeposited cohesive sediment clasts eroded from the underlying sub-layer (ESL). DL has occasionally a sharp lower boundary. The thinner upper part of the DL consists of a finer detrital grains matrix containing in some cases thin coarser non-annual intercalated layers. The DLs are associated with higher density values (Fig. 4) and an increase in the abundance of elements Sr and Ca (Zolitschka et al., 2015). Few organic debris and charcoal fragments are observed throughout the DLs. The third topmost varve sub-layer is formed by a fine to medium silty layer with abundant clay rich in Fe and interpreted as an Autumn and Winter Layer (AWL), also known as a clay cap (Zolitschka et al., 2015). The Fe peak values in AWLs are hence

https://doi.org/10.5194/cp-2020-87
Preprint. Discussion started: 20 July 2020

Climate of the Past
Discussions
Open Access

used to determine the upper varve boundary (Fig. 4) (Zolitschka et al., 2015) as previously performed in other varved sequences (Cuven et al., 2010; Saarni et al., 2016).

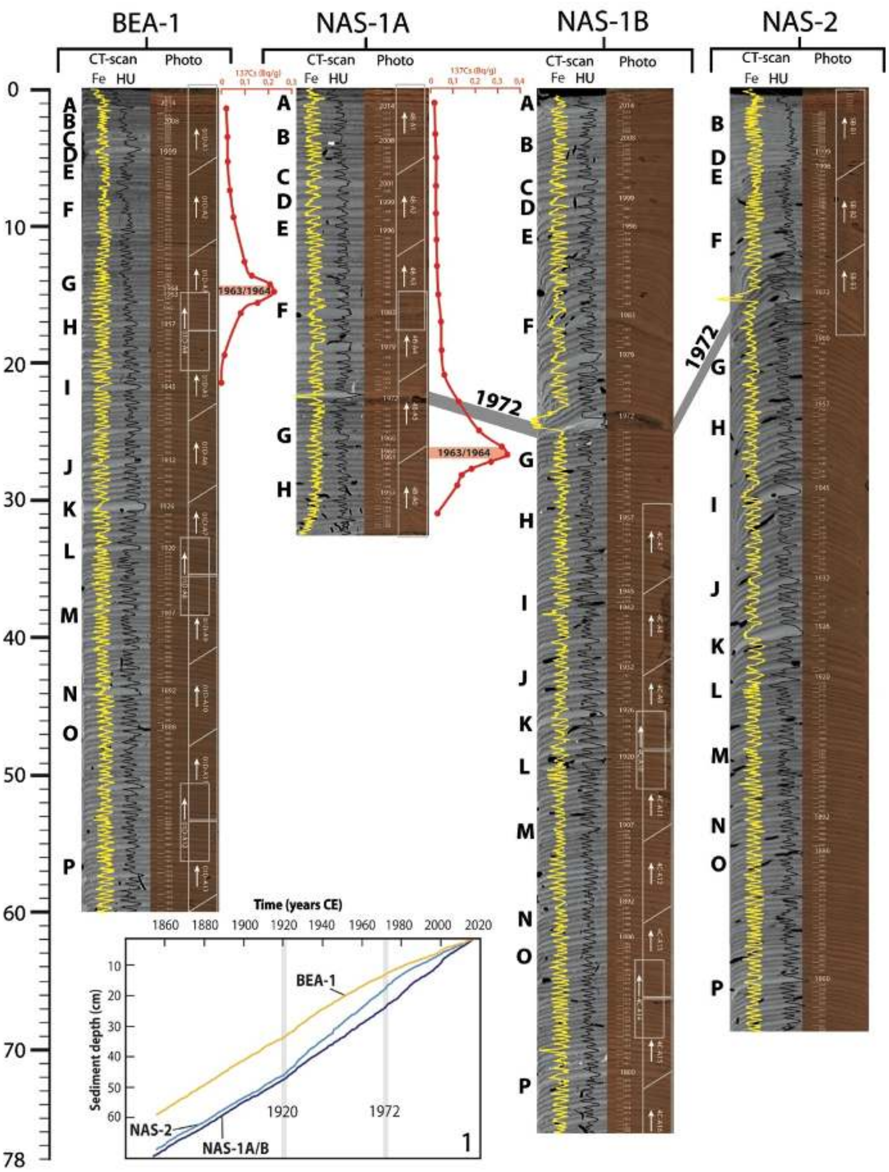

Figure 4. Varve counts made on (left) CT-scan and (right) high resolution images from core BEA-1, NAS-1A/B and NAS-2. Distinctive marker layers are identified by letters A to P. The 1972 CE marker layer is outlined by the thick dark gray line. Fe abundance and density (HU) profile represented by the yellow and black line respectively, show rhythmic laminations. The activity profile of ^{137}Cs in core BEA-1, NAS-1A is shown by the red line. Approximate thin-section locations are outlined by white boxes. The age-depth model of the 3 cores is also presented (Box. 1). See Fig. 1b for core locations.

https://doi.org/10.5194/cp-2020-87
Preprint. Discussion started: 20 July 2020

The lamination deposited in 1972 CE from sites in the axis of the Naskaupi River (NAS-1; Fig. 5b and NAS-2; Fig. 4), present a thick and coarse DL composed of very fine sandy and very coarse silt (Fig. 5) representing the highest particle size measured in all sequences. Furthermore, there is a difference in varve properties and microfacies deposited before and after the 1972 CE marker bed, especially in core NAS-1, the proximal site from the Naskaupi river mouth. Varves deposited prior 1972 CE have a well-developed substructure relatively constant among each annual lamination (Fig. 5b). The ESL of the pre-1972 CE varves is thicker and more clearly visible. Conversely, the DL of varves post-1971 CE is thicker, while the ESL is more difficult to discern and contributes less to the TVT (Fig. 5a). The ESL in varve post-1971 CE from sites NAS-1 and NAS-2 no longer contains isolated coarse debris. The changes in varve facies are less noticeable in core NAS-2, which was sampled further away from the Naskaupi River mouth. The 1972 CE marker bed and related facies changes are not found at the Beaver River mouth site BEA-1.

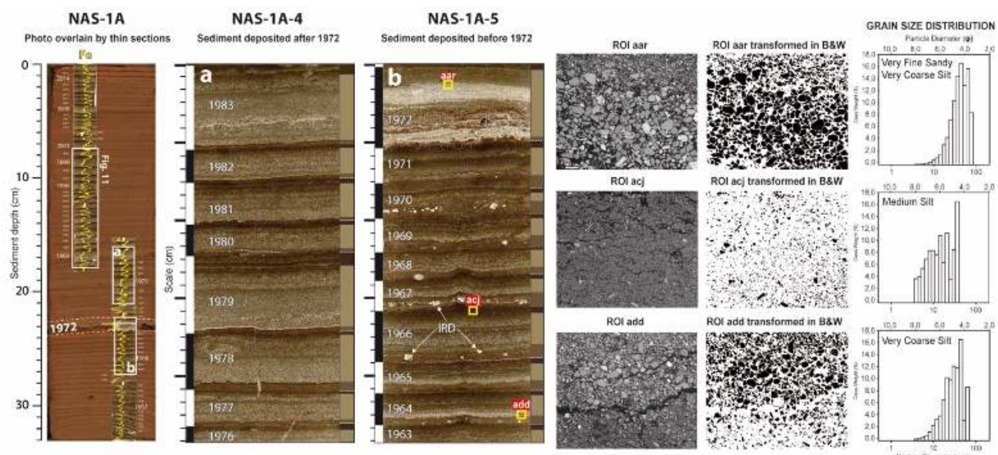

Figure 5. (Left) Photo of core NAS-1A overlain by thin-section image and Fe abundance profile (yellow lines). The 1972 CE marker layer is outlined by the white dashed lines. Thin section images showing sedimentary structure of varves deposited (B) before and (A) after the 1972 marker bed. Varve boundaries are represented by the vertical black and white bars. Varve sub-layers are delimited by the medium brown (ESL), pale brown (DL) and dark brown (AWL) bars. Typical IRD are shown by the white arrows on the b panel. (Right) BSE images of three ROIs transformed in B&W and their associated particle-size distribution (aar: the 1972 CE marker layer; acj: a typical AWL; add: the base of a typical DL) (see yellow squares on the b panel for ROIs location).

4.2 Varve chronology

The varve chronologies are consistent with the Cesium-137 main peaks corresponding to the highest atmospheric nuclear testing period (1963-1964 CE) (Appleby, 2001). Peaks are found at 14-14.5 cm (BEA-1) and 26.5-27 cm (NAS-1A) depth (Fig. 4) and perfectly match the lamination counts in both cores, confirming the varve assumption. Also, the 1972 CE thick and coarse stratigraphic marker observed the year after the anthropogenic modification of the watershed for hydropower generation, supports the reliability of the constructed chronologies.

Independent varve chronologies were established from sediment cores BEA-1, NAS-1 and NAS-2 (Fig. 4). A total of 160 varves were counted at each site, covering the 1856-2016 CE period. The thickness and the good quality of the preserved varve structures allowed to build a robust age-model reproducible among cores. Despite the significant distance between the coring sites (1 to 5 km) and the two different sediment sources (Naskaupi and Beaver River) (Fig. 1b), there is no varve counts difference between the established thick marker layers (A to P; Fig. 4) among cores. The few counting difficulties occur within varve years 1952-1953, 1935-1934, 1918-1919, as it contains ambiguous coarse non-annual intercalated layers with intermediate clay cap that can be interpreted as one year of sedimentation. The age-depth models (Fig. 4, Box. 1) show changes in sediment accumulation rates (thickness) among cores in 1920 and 1972.

4.3 Thickness and particle size measurements

The TVTs from core BEA-1, NAS-1 and NAS-2 vary between 0.95 and 12.91 mm, with an average thickness of 4.09 mm (Fig. 6a, b, c). The DLTs vary between 0.29 and 8.3 mm, with an average thickness of 1.9 mm. There are significant strong positive correlations between TVT and DLT for each core ($r = 0.79$ to 0.91; $p < 0.05$). Since the 1920s, TVTs and DLTs from core BEA-1 have decreased slowly until 2016 (fig. 6a). A step in the TVT is observable in the early 1920s at the three sites (Fig. 6a, b, c), especially in core NAS-2, which recorded their highest values during the 1920-1972 period (Fig. 6c). From 1920 to 1972, the mean TVT series show a slight downward trend, despite an increase in years associated with high thickness values (Fig. 6b, c). The mean DLT series does not show a

https://doi.org/10.5194/cp-2020-87
Preprint. Discussion started: 20 July 2020

clear trend. TVT and DLT vary similarly in time between sites for the 1856-1971 period (Fig. 6d, e). However, after 1972, TVT and DLT series are more diverging. From 1972 to 2016, TVT and DLT have declined in cores BEA-1 (Fig. 6a) and NAS-2 (Fig. 6c), and the amplitude of their variability tends to diminish. For core NAS-1 (Fig. 6b), this period is associated with high thickness values. Core NAS-1 has recorded a slight TVT and DLT decrease for the 1972-2016 period, but unlike the other cores, the variability tends to increase with time.

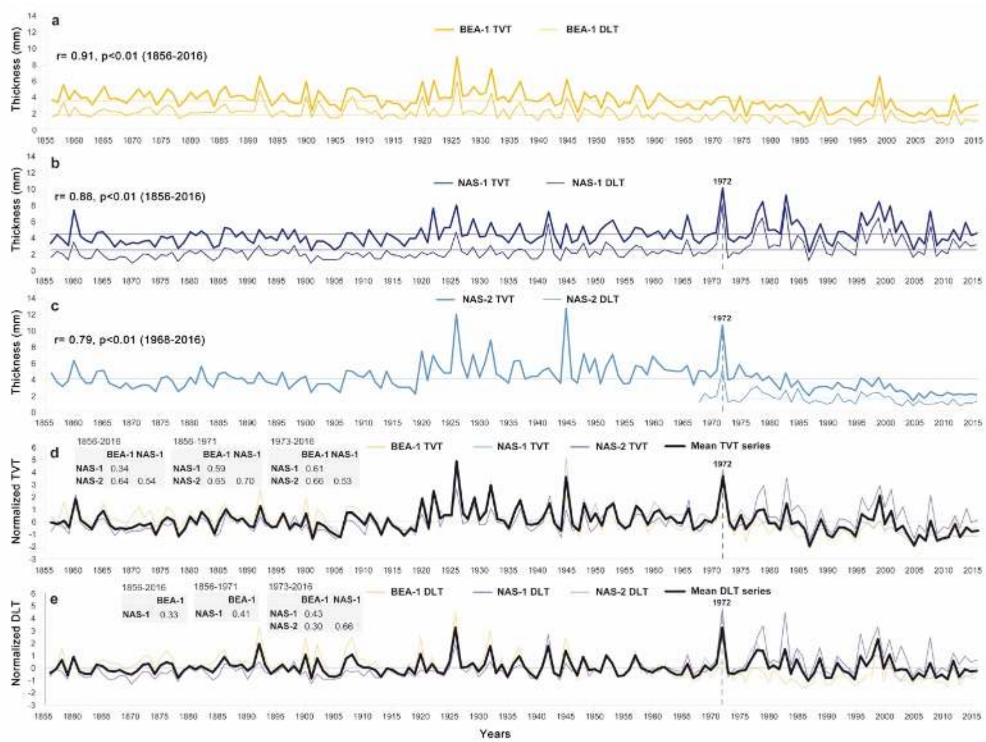

Figure 6. Total Varve Thickness (TVT; thick line) and Detrital Layer Thickness (DLT; thin line) time series of core (a) BEA-1, (b) NAS-1 and (c) NAS-2. Comparison of normalized (d) TVT and (e) DLT series and the mean TVT and DLT series. Pearson correlation coefficients between TVT and DLT for the 1856-2016, 1856-1971 and 1973-2016 periods are shown. The 1972 CE marker layer is outlined by the black dashed line.

The $P99D_0$ (Fig. 7) yields the strongest correlations with instrumental data. There is weak to moderate positive correlation between TVT and $P99D_0$ from a same core (BEA-1: $r = 0.12$ $p > 0.05$; NAS-1: $r = 0.52$ $p < 0.05$; NAS-2: $r = 0.27$, $p > 0.05$). The correlation between DLT with $P99D_0$ is stronger (BEA-1: $r = 0.15$ $p > 0.05$; NAS-1: $r = 0.65$ $p < 0.05$; NAS-2: $r = 0.49$, $p < 0.05$).

https://doi.org/10.5194/cp-2020-87
Preprint. Discussion started: 20 July 2020

Climate of the Past Discussions
Open Access

The $P99D_0$ of cores BEA-1, NAS-1 and NAS-2 vary between 20 and 67.7 µm, with an average value of 34.3 µm (Fig. 7). The mean $P99D_0$ series show a slight coarsening trend towards the end of the 19th century. From 1900 to 1971, $P99D_0$ values are generally below average. The 1972 marker bed of core NAS-1 presented the maximum $P99D_0$ values (Fig. 7a). After 1972, there is an increase of $P99D_0$ values especially in core NAS-1, where a step is observable.

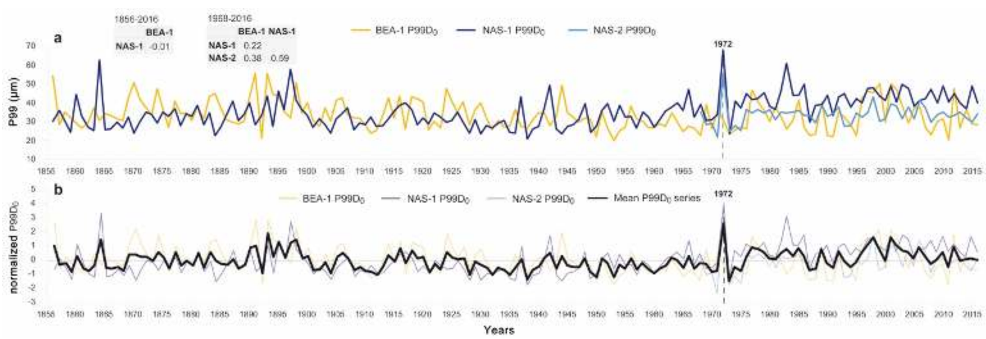

Figure 7. (a) $P99D_0$ time series of cores BEA-1, NAS-1 (1856-2016) and NAS-2 (1968-2016). Pearson correlation coefficients between $P99D_0$ series for the 1856-2016 and 1968-2016 periods are shown. (b) Comparison of normalized $P99D_0$ series and the mean $P99D_0$ series. The 1972 CE marker layer is outlined by the black dashed line.

4.5 Relation between varve series and instrumental record

To examine how the physical parameters of the varves are related to local hydroclimate and to demonstrate their potential for hydrological reconstruction, sediment parameters (TVT, DLT and PSI) of each core were systematically compared to hydrological variables (Tab. 1). TVT, DLT and $P99D_0$ series from the three coring sites show significant positive correlations with the Q-mean and Q-max extracted from the Naskaupi River hydrometric station (03PB002) data on the 1978-2011 period (n=31) (Tab. 3). The TVT and DLT of cores BEA-1 and NAS-2 show stronger correlation with Q-mean, while TVT and DLT of cores NAS-1 have a better relation with Q-max. There is a significant negative correlation between $P99D_0$ of core NAS-1 and Q-Max-JJ ($r = -0.38$) and Rise-Time ($r = -0.47$). Sediment parameters also present significant positive correlations with E-QNival ($r = 0.38$ to 0.63), Snow-Win ($r = 0.40$ to 0.61) and Nb-days-SupQ80 (> 125 $m^3 \cdot s^{-1}$) ($r = 0.27$ to 0.60). Moreover, the $MaxD_0$ series of core NAS-1 show significant ($p < 0.01$) positive correlations with the average spring temperature ($r = 0.40$; not shown in Tab. 3).

https://doi.org/10.5194/cp-2020-87
Preprint. Discussion started: 20 July 2020

DLT, TVT and $P99D_0$ data from core BEA-1 (1856-2016), NAS-1 (1856-2016) and NAS-2 (1968-2016) have been normalized and averaged to produce mean TVT, DLT and $P99D_0$ series (Fig. 6d, e; 7b). Mean TVT, DLT and $P99D_0$ series were also compared with hydrological variables (Tab. 3). The 1972-2016 measurements of NAS-1 were excluded from the mean DLT series since due to the suggested anthropogenic impact on sedimentation during this period. Moreover, mean correlations between the mean DLT series with hydrological variables are stronger without the 1972-2016 period (adj R^2: 0.47 vs 0.34). The comparison made with mean DLT and $P99D_0$ series yields the strongest correlations in our dataset ($r = 0.69$ and 0.76; Tab. 3) and have been used to reconstruct local Q-mean and Q-max respectively (Fig. 8).

To determine if there is a regional hydrological signal in Labrador and whether the Grand Lake varved sedimentary sequence has recorded this signal, the Naskaupi River hydro-climatic variables were compared with other Labrador hydrometric stations. Good relation exists between the Naskaupi River hydro-climatic variables and other Labrador hydrometric stations (Fig. 3, Tab. 2). For instance, the instrumental Naskaupi River mean annual discharge series data show significant ($p < 0.01$) strong positive correlations with other stations (Ugjoktok: $r = 0.84$; Minipi: $r = 0.70$; Little Mecatina: $r = 0.73$; Eagle: $r = 0.49$). Therefore, the mean DLT series has been used to reconstruct mean annual discharges for the Labrador region (Fig. 9).

https://doi.org/10.5194/cp-2020-87
Preprint. Discussion started: 20 July 2020

Table 1. Extract of the Matrix of correlation coefficients (Pearson r) of the hydro-climatic variables defined in Tab. 1 with Total Varve Thickness (TVT), Detrital Layer Thickness (DLT) and Particle Size ($P99D_0$) on the instrumental period (1978-2011; n=31) for each core. Correlations between the hydro-climatic variables and the mean TVT, DLT and $P99D_0$ series (normalized and averaged varve parameters of cores BEA, NAS-1 and NAS-2) are also present. Correlations in Boldface are significant at $p < 0.05$. Correlations marked by an asterisk were used for the final Q-mean and Q-max reconstructions.

Sediment parameters		Hydroclimatic variables of station 03PB002						
	Core BEA-1	**Q-mean**	**Q-max**	**Q-max-JJ**	**Rise-Time**	**Nb-days-supQ80**	**E-Qnival**	**Snow-Win**
	TVT	**0,53**	**0,46**	-0.08	-0.05	**0.50**	**0.41**	**0.45**
	DLT	**0,54**	**0,38**	-0.009	0.22	**0.49**	0.32	0.29
	$P99D_0$	**0,56**	**0,56**	-0.05	0.16	**0.38**	**0.40**	**0.27**
	Core NAS-1	**Q-mean**	**Q-max**	**Q-max-JJ**	**Rise-Time**	**Nb-days-supQ80**	**E-Qnival**	**Snow-Win**
	TVT	**0.52**	**0,64**	-0,30	-0,26	**0,48**	**0,56**	**0,54**
	DLT	**0.52**	**0,67**	-0,31	-0,27	**0,51**	**0,54**	**0,48**
	$P99D_0$	0.18	**0,60**	**-0,38**	**-0,47**	0,23	**0,40**	**0,32**
	Core NAS-2	**Q-mean**	**Q-max**	**Q-max-JJ**	**Rise-Time**	**Nb-days-supQ80**	**E-Qnival**	**Snow-Win**
	TVT	**0,60**	**0,55**	**-0,20**	-0,24	**0,63**	**0,44**	**0,57**
	DLT	**0,62**	**0,57**	0,07	-0,13	**0,50**	**0,61**	**0,60**
	$P99D_0$	**0,39**	**0,43**	**0,19**	0,26	**0,37**	**0,40**	0,12
	Mean series	**Q-mean**	**Q-max**	**Q-max-JJ**	**Rise-Time**	**Nb-days-supQ80**	**E-Qnival**	**Snow-Win**
	TVT	**0,57**	**0,61**	-0,27	-0,21	**0,55**	**0,52**	**0,55**
	DLT	**0,69***	**0,59**	-0,01	-0,02	**0,59**	**0,56**	**0,57**
	$P99D_0$	**0,58**	**0,76***	-0,10	0,03	**0,49**	**0,57**	**0,33**

4.6 Hydrological reconstructions

The Naskaupi River mean and maximum annual discharges (Q-mean and Q-max; Fig. 8) as well as the Labrador region mean annual discharges (Regional Q-mean; Fig. 9) were reconstructed from the mean DLT and $P99D_0$ series for the 1856–2016 period. Due to the suggested anthropogenic origin, the varve of the year 1972 is considered as an outlier and thus was not included for reconstruction. The cross-validation method demonstrates the quality of the reconstructions. The adj R^2 of the two calibrated periods are significant ($p < 0.0001$) and the RE and CE of the verification periods are > 0 which validates the model skills (Fig. 8, 9). The significant correlation between reconstructed Q-mean and Q-max values and observed discharge data validates the predictive capacity of the model.

The reconstructed Naskaupi River Q-mean from mean DLT series varies between 78 and 146 $m^3 \cdot s^{-1}$, with an average of 95 $m^3 \cdot s^{-1}$ (Fig. 8a), and remains relatively stable from 1856

https://doi.org/10.5194/cp-2020-87
Preprint. Discussion started: 20 July 2020

to 1925, mainly near average. Several years with high Q-mean occurred during the 1925-1960 period. There has been a slight statistically significant downward trend of the Q-mean over the last 90 years. Recently, high Q-mean periods are observed from 1976 to 1985 and 1996 to 2002 and lower Q-mean periods from 1986 to 1995 and 2003 to 2016. The reconstructed Naskaupi Q-max from $P99D_0$ series varies between 226 and 695 $m^3 \cdot s^{-1}$, with an average of 426 $m^3 \cdot s^{-1}$ (Fig. 8b). There is a slight upward trend in Q-max at the end of the 19th century. The 1900-1971 period is characterized by a Q-max generally below average. Three periods of high Q-max are observed from 1887-1991, 1976 to 1986 and 1995 to 2008 (Fig. 8b). While some caution should be applied when comparing pre- to post 1972 reconstructions, given the changes in watershed conditions that happened after the construction of the system of dykes. The good relation between mean DLT series and the observed Labrador region Q-mean series (Fig. 9), based on the discharge variability of five watersheds of different size and location, demonstrates that the Grand Lake varved sequence is robust and contains a regional signal.

4.7 Comparison with the rainfall-runoff modeling approach

Naskaupi River Q-mean and Q-max were also reconstructed using the ANATEM rainfall-runoff modeling (Fig. 10). These reconstructions are statistically and positively correlated with the yearly time series obtained from varves properties during the 1880-2011 period (Q-mean: $r = 0.37$; Q-max: $r = 0.22$; $n = 131$; $p < 0.05$). The reconstructed Q-mean and Q-max annual variabilities show similarities, especially during the 1973–2011 period (Q-mean: $r = 0.54$; Q-max: $r = 0.34$; $n = 43$).

Q-Mean reconstructions with both varves properties and modeling are better correlated than the Q-Max reconstructions. This may be due to the higher uncertainty related to the Q-max reconstruction with the modeling approach. Indeed, high flow modeling requires good reconstruction performances on several hydro-climatic processes (i.e. snow accumulation during the winter, timing of the snowmelt, spring precipitation). Moreover, the uncertainty of the hydrological reconstruction is less important on recent periods (>1950), due to the better quality of the geopotential height fields reanalysis over recent decades, as more stations series are available and thus used in the reanalysis. The decrease

https://doi.org/10.5194/cp-2020-87
Preprint. Discussion started: 20 July 2020

Climate of the Past
Discussions
Open Access

in the uncertainty related to reanalysis over time might explain the better correlation between the two approaches on the recent period.

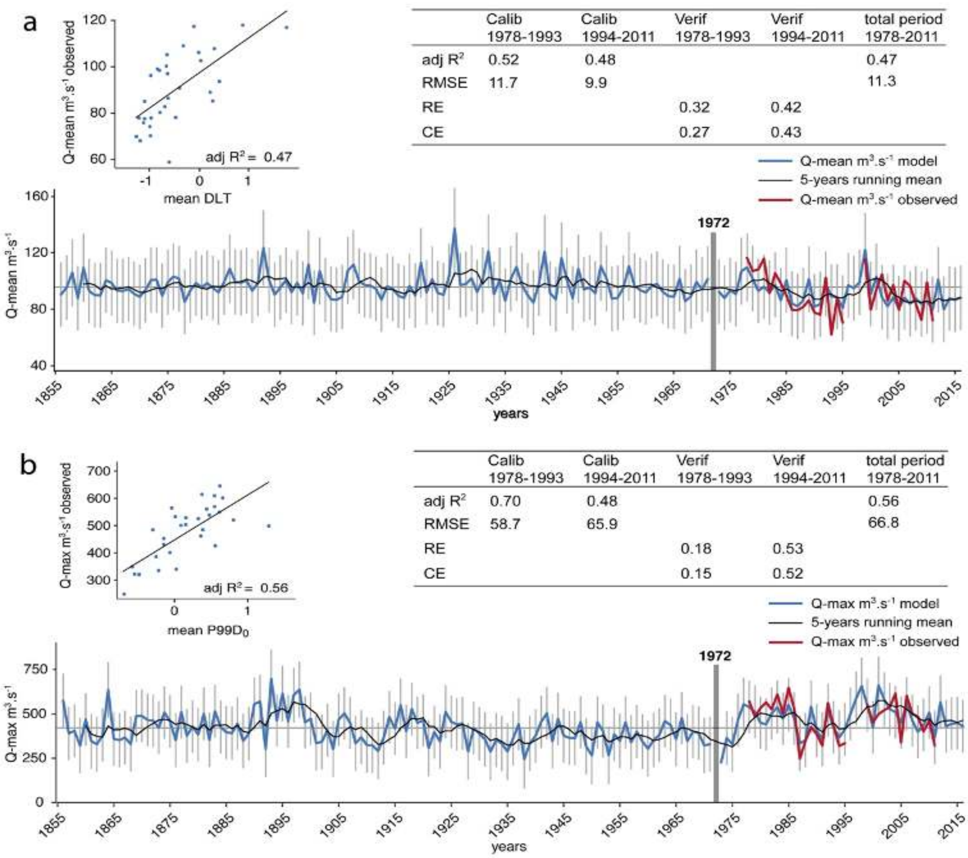

Figure 8. Local (a) Q-mean and (b) Q-max reconstructed from the mean DLT and $P99D_0$ series respectively, for the 1856–2016 period (blue line), with 5-year moving average (black line). Error bars represent the 95% confidence interval. Observed Q-mean and Q-max are also shown for the 1978-2011 period (red line).

https://doi.org/10.5194/cp-2020-87
Preprint. Discussion started: 20 July 2020

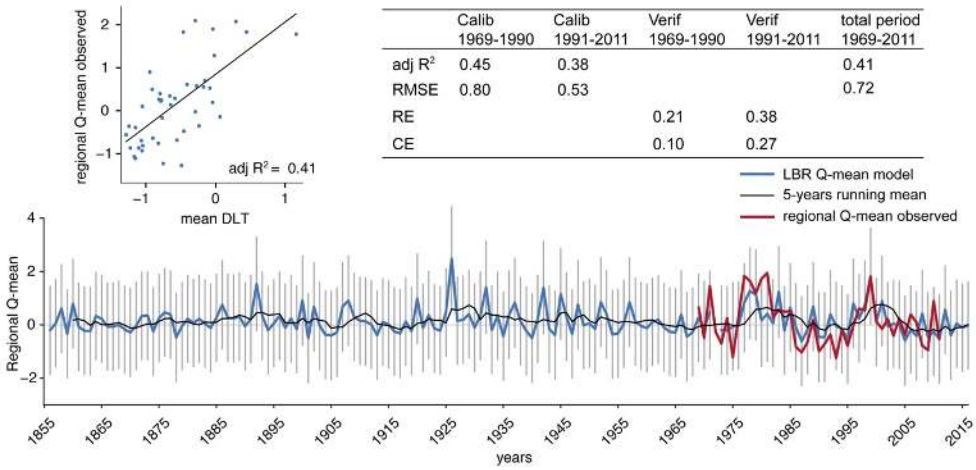

Figure 9. Labrador region Q-mean reconstructed from the mean DLT series for the 1856–2016 period (blue line), with 5-year moving average (black line). Error bars represent the 95% confidence interval. Observed Labrador region Q-mean series is also shown for the 1969-2011 period (red line).

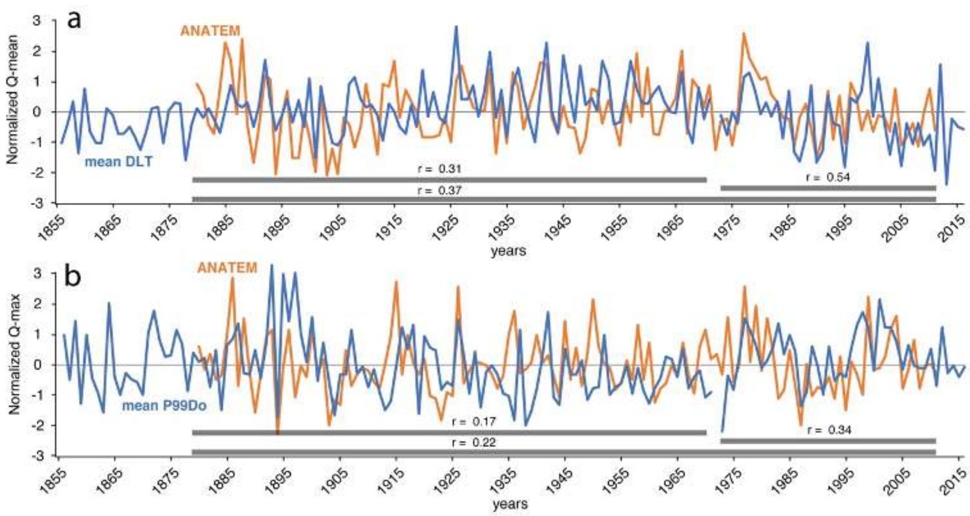

Figure 10. Comparison between (a) Q-mean and (b) Q-max reconstruction using varve (blue line) and the rainfall-runoff modeling (orange line) for raw yearly data.

https://doi.org/10.5194/cp-2020-87
Preprint. Discussion started: 20 July 2020

5. Discussion

5.1 Grand Lake varve formation

Lakes containing well-defined and continuous varved sequences that allow the establishment of an internal chronology are rare in boreal regions. However, the great depth of Grand Lake, the availability of fine sediments in its watershed due to the glacial and postglacial history of the region (Trottier et al., 2020), as well as its important seasonal river inflow have favored the formation and preservation of varved sediment. The seasonal streamflow regime plays a significant role in the annual cycle of sedimentation in Grand Lake and is responsible for the formation of the three distinct varve sub-layers. Due to the important thickness and the clarity of the varve structures, it is possible to infer the deposition mechanism of these sub-layers and the season in which they were deposited.

The ESLs are interpreted to be deposited during the river and lake ice break-up and disintegration period, when erosion and resuspension of fine-grained sediments are initiated. Available Landsat-8 images of Grand Lake covering the 1983-2018 period (courtesy of the U.S. Geological Survey) shows that Grand Lake ice cover starts to melt at the Naskaupi and Beaver river mouths. This ice melting pattern creates open bays where drifting floating ice melts thus depositing ice rafted debris (IRD) (Lamoureux 1999, 2004) as observed in the ESL facies. The underlying DLs are interpreted as flood-induced turbidites deposited at the lake bottom during the open-water season. High energy sediment-laden river flows produce hyperpycnal flows allowing silt and sand-size sediments to reach the cored sites (Cockburn and Lamoureux, 2008). Seldom traces of erosion at the top part of the ESL support the hypothesis that the DLs originated from these underflows (Mangili et al., 2005). The sediment waves on the Naskaupi and Beavers river delta slopes (Trottier et al., 2020) (Fig. 1b, c) also indicates significant downstream sediment transport by supercritical density flows (Normandeau et al., 2016). The thick and grading upward basal part of the DLs are deposited during the high spring discharge period generated by snowmelt runoffs. In spring, river discharge reaches its annual peaks and sediment transport capacities, that are then no longer reached during the rest of the summer and autumn (Fig. 2, 11). However, the presence of thin coarser non-annual intercalated layers in the upper part of the DL indicates that some rainfall events, as observed in Fig.

https://doi.org/10.5194/cp-2020-87
Preprint. Discussion started: 20 July 2020

11 (i.e. 1983, 1987, 1992, 1999) also contribute to deposition of sediments in this sub-layer. The overlying AWL resulted from the settling and flocculation of fine particles in non-turbulent condition from fall through the onset of lake ice, forming a typical clay cap.

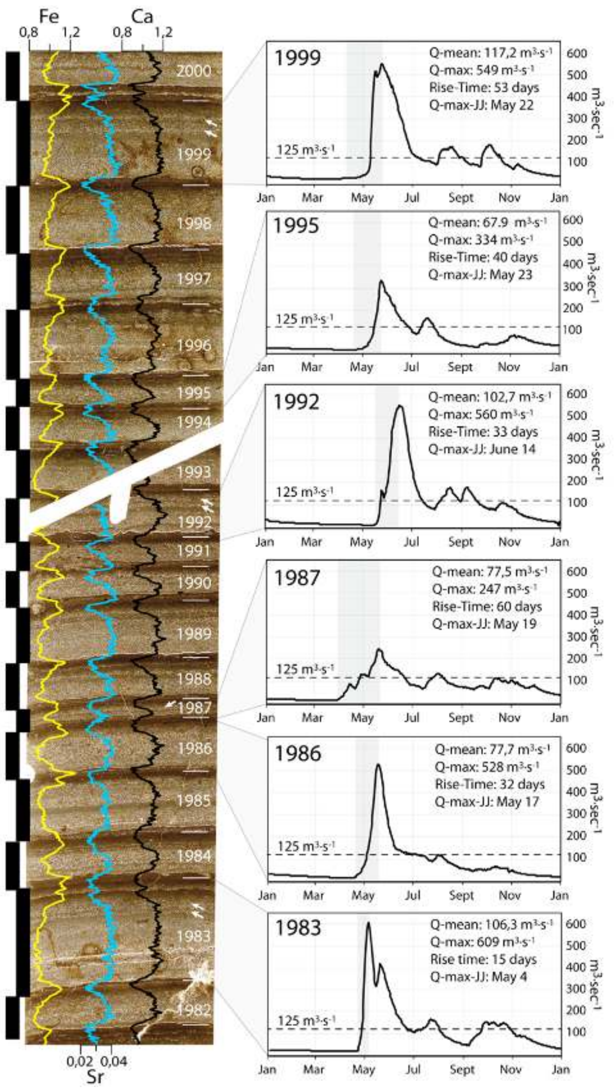

Figure 11. Qualitative comparison between NAS-1A varves from thin sections (delimited by the black bars) with the hydrographs of the Naskaupi River. Observed annual Q-mean and Q-max as well as the timing and rise time of the peak spring discharge are shown. Black dotted lines represent the discharge threshold of ~125 $m^3 \cdot sec^{-1}$. (1999, 1992, 1986, 1983) Strong spring floods associated with thick coarse varves. (1995, 1987) Low spring floods associated with thin varves. (1999, 1992, 1987, 1983) Coarser intercalated layers in the upper part of the DL linked with summer and autumn high-discharge events. (1986) Strong spring flood with a low summer and autumn flow associated to a varve without substructure. Thin sections are overlain by iron (Fe: yellow line), strontium (Sr: blue line), and calcium (Ca: black line) abundances. See Fig. 5 for thin sections locations.

https://doi.org/10.5194/cp-2020-87
Preprint. Discussion started: 20 July 2020

5.2 Anthropogenic influences on recent sedimentation

Anthropogenic environmental impacts on watersheds can be preserved in varved lake sediments (Zolitschka et al., 2015; Saarni et al., 2016; Czymzik et al., 2018). The well-developed sub-layers of Grand Lake varves deposited prior to 1972 CE from sites NAS-1 (Fig. 6b) and NAS-2, and the similarity between TVT and DLT values and variations among all sites over the 1856-1971 period (Fig. 6d) indicate that before the Naskaupi River diversion, seasonal sedimentation cycles appear to have reached a relative state of equilibrium. River sediment input seems to have been quantitatively and spatially constant. The 1972 CE marker bed shows that the river dyking had an abrupt impact on sedimentation in Grand Lake the year following the diversion. The spring/summer/autumn flood(s) of the years 1972 CE has (have) remobilized newly available sediments and deposited a thick and coarse-grained turbidite on the lake floor in the axis of the Naskapi river. The reduction of nearly half of the area of the Naskaupi River watershed reduced the water inflows and changed the base level of the downstream river system. The rapid base level fall must have triggered modifications of the fluvial dynamics such as channel incision, banks destabilization and upstream knickpoint migration, likely increasing the availability of sediments in the River system. The important thickness and high grain size values of varves deposited post-1971 in core NAS-1 (Fig. 5a, 6d/e, 7b, 11) show that the diversion has affected sedimentation at this site over time. During the 1972-2016 period, the Naskaupi River floodplain sediments must have been in a re-equilibration phase favorable to erosion, sediment transport, and deposition on the delta slope. The thin ESLs free of IRD in varve post-1971 of core NAS-1 (Fig. 5a, 11) and NAS-2 indicate that early spring discharge has less capacity for transport fine sediments and lost its ability to float ices to Grand Lake due to the decrease in water supplies.

It is also tempting to link the decrease of varve thickness in core NAS-2 over the 1972-2016 period to the Naskaupi River diversion. However, similarities with core BEA-1, a site devoid of anthropogenic perturbations (unaffected by the Naskaupi River diversion) which also shows a decline in varve thickness, suggest that this decrease can be potentially due to a natural hydro-climatic signal. Indeed, because of the distant location of site BEA-1 from the Nakaupi River mouth, the diversion is most likely not responsible for the decrease

https://doi.org/10.5194/cp-2020-87
Preprint. Discussion started: 20 July 2020

of varve thickness in this sector. Moreover, it is quite unlikely that the sedimentary input from the Naskaupi River contributed to sediment accumulation at the mouth of the Beaver River. The absence of any traces of the 1972 CE marker bed at the Beaver River mouth (BEA-1) supports this hypothesis. Furthermore, the thickness decrease observed in BEA-1 began after 1925 (Fig. 6a) which is before the 1971 diversion.

Anthropogenic modification of the Naskaupi watershed makes it challenging to determine natural hydroclimate-related changes after 1971. Several core section combinations including or excluding the 1972-2016 period were thus compared to the hydrological variables, in order to elaborate the most relevant mean DLT and $P99D_0$ series for reconstructions. The 1972-2016 period of NAS-1 was excluded from the mean DLT series used to reconstruct local and regional Q-mean, the reason being that this proximal site has become more sensitive to maximum discharges in spring than mean annual discharges since the diversion. Indeed, best result (adj R^2: 0,56 vs 0,34) was obtained by keeping this period in the mean $P99D_0$ series used to reconstruct local Q-max. The negative correlation between $P99D_0$ of the NAS-1 and the timing and rise time of spring discharge (Table 3) also demonstrates reactivity to spring entrainment energy conditions.

5.3 The hydro-climatic signal in the varve record

Cross correlations between varve parameter series (1856-2016) with instrumental data (1969-2011) and rainfall-runoff modeling reconstructions (1880-2011) show no lag, which demonstrates the accuracy of the time series used in this study. The good correlations between continuous varve thickness and grain size measurements with instrumental hydrological variables (Tab. 3) show that Grand Lake varved sediments are reliable proxies to reconstruct past hydrologic conditions through time at the annual scale. The thick and/or coarse-grained varves correspond well to years of high river discharges, whereas thin and/or fine-grained varves are related with years of low discharge. The pooling of varve parameters from different coring sites linked to separate sediment sources (Fig. 1b) for the establishment of the normalized mean series, improved the correlations with hydrological variables (Tab. 3) and thereby the reconstruction results (Fig. 8, 9). The use of mean series

https://doi.org/10.5194/cp-2020-87
Preprint. Discussion started: 20 July 2020

Climate of the Past
Discussions

is likely attenuating the local particularities of each site, providing a more global hydro-climatic signal than individual core.

As demonstrated by previous studies on varved sediments, the use of both VT and PSI allows for a more specific investigation of the range of hydroclimate conditions recorded within varve (Francus et al., 2002; Cockburn and Lamoureux, 2008; Lapointe et al., 2012). For Grand Lake, the mean DLT is found to be the best proxy to reconstruct all hydrological events occurring throughout the year (Q-mean). The best result obtained with DLT instead of TVT for the final Q-mean reconstructions might be explained by the slight variability of ESLs and AWLs thickness included in the TVT measurements. This variability can be linked to specific climatic and geomorphological parameters such as the duration of ice cover on Grand Lake and the Naskaupi River ice breakup processes which induce noise in the hydrologic signal contained in TVT series. The SLs and AWLs thickness variability is the reason why the step in the TVT in the early 1920s (Fig. 6d) is less perceptible in the DLT series (Fig. 6e). The ESLs and AWLs both show high thickness values during this period. The mean $P99D_0$ yields the strongest correlation in our dataset (Tab. 3) and is then the robust proxy used to reconstruct maximum annual discharges (Q-max). Moreover, this indicator is not sensitive to compaction, which may affect other proxies based on thickness. Reconstructed Q-max series reveals more significant interannual and decadal variability.

The good relations between sediment parameters and Snow-Win, E-Qnival and even Temp-Spring (Tab. 3), demonstrate that Grand Lake varve predominantly reflects spring discharge conditions (e. g. Ojala and Alenius 2005; Lamoureux et al., 2006; Saarni et al., 2016; Czymzik et al., 2018), which is the major component of the regional streamflow regimes classified as nival (snowmelt-dominated) (Bonsal et al., 2019). In boreal regions, the intensity and length of spring floods are controlled by the snow accumulation during winter and by the temperature of the melting period (Hardy et al., 1996; Snowball et al., 1999; Cockburn and Lamoureux, 2008; Ojala et al., 2013; Saarni et al., 2017). The negative correlation between $P99D_0$ of the NAS-1 and the timing and rise time of spring discharge suggests that early spring flows that increase rapidly are conducive conditions for high entrainment energy and the deposition of coarser laminations on the distal part of the delta

https://doi.org/10.5194/cp-2020-87
Preprint. Discussion started: 20 July 2020

slope (Fig. 11; site NAS-1). The erosion of detrital materials in early spring increases when the snowmelt runoffs occur on soils that are not yet stabilized by vegetation (Ojala and Alenius 2005, Czymzik et al., 2018).

Despite the presence of sporadic non-annual intercalated layers in the top part of the DL interpreted to be produced by summer or fall rainfall events (Fig. 11), there is non-significant low correlations between varves and Ptot-Annual/Ptot-Sum (not shown). These intercalated layers suggest that rainfalls have a minor contribution in the thickness and especially in the varve grain size, as the coarsest particles are found at the base of the DL. The relations between varve parameters and Nb-days-SupQ80 suggests that a daily discharge of ~125 $m^3 \cdot s^{-1}$ represents an approximate threshold above which the deposition of coarse sediment in Grand Lake (DLs) is more likely (Fig. 11) (e.g., Czymzik et al., 2010). According to the instrumental data (Fig. 2, 11), such a discharge can be generated during the summer/autumn period, suggesting that rainfall events are indeed responsible for the formation of thin intercalated layers sometimes observed at the top of the DLs (Fig. 11).

The correlations between the Naskaupi River hydro-climatic variables and other Labrador hydrometric stations (Fig. 3) show that a coherent regional hydrological pattern exists in the Labrador region. The performed regional Q-mean reconstitution and validation (Fig. 9) indicated that the Labrador region hydrologic signal is recorded in Grand Lake varve sequence. The local and regional Q-mean reconstructed from mean DLT series suggest slight decrease in mean annual discharge during the last 90 years. Q-mean and Q-max reconstructions based on both varve series and rainfall-runoff modeling revealed high value periods from 1975 to 1985 and 1995 to 2005, and low values from 1986 to 1994 and 2006 to 2016 (Fig. 10). These results agree with the downward trend of the annual streamflow observed in eastern Canada during the 20th century and also with higher river discharges from 1961 to 1979 and 1990 to 2007, and lower discharges from 1980 to 1989 (Zhang et al. 2001; Sveinsson et al., 2008; Jandhyala et al., 2009; Déry et al., 2009; Mortsch et al., 2015; Dinis et al., 2019).

In addition to providing the first Late Holocene varved record in eastern Canada, these results highlight the complementarity between palaeohydrological data extract from varved sediments and rainfall-runoff modeling as well as offering a centennial perspective on river discharges variability in an important region for the economic and sustainable development of water resources in Canada. Reconstructed long-term mean and maximum annual river discharges series provide valuable quantitative information particularly for water supply management for hydropower generation and the estimation of flood and drought hazards. This research also allows documenting the effect of dyke systems on the downstream sediment transport dynamic into a watershed and its implication for palaeohydrological reconstruction. Further investigation of the impacts of the Naskaupi watershed reduction on sediment transport could help to better our reconstructions. Future work in Grand Lake should be directed towards the high-resolution analysis of long sediment cores in order to produce longer reconstructions. The Grand Lake deeper varved sequence potentially recorded the hydro-climatic variability that occurred during the Late Holocene in a key region for the North Atlantic climate study. Additional research is needed to determine whether large-scale atmospheric and oceanic variability modes influence river discharge in the Labrador region.

6. Conclusions

The great depth of Grand Lake, the availability of fine sediments along its tributaries, and its important seasonal river inflow have favored the formation and preservation of fluvial clastic laminated sediments record. By using the first Late Holocene varved record in eastern Canada and a rainfall-runoff modeling approach, this paper provides a better understanding of the recording of hydro-climatic conditions in large and deep boreal lakes and allows extending the hydrological record beyond the instrumental period as well as the spatial coverage of the rare annual palaeohydrological proxies in North America. The key results of this study are:

- The annual character of the 160 years-long lamination sequence has been confirmed. Each varve, composed of an early spring layer, a summer/autumn detrital layer and an autumn and winter layer, represents one hydrological year.

https://doi.org/10.5194/cp-2020-87
Preprint. Discussion started: 20 July 2020

- Grand Lake varve formation is mainly related to the largest hydrological event of the year, the spring discharge, with minor contributions from summer and autumn rainfall events.
- Two hydrological parameters, Q-mean and Q-max annual discharges, are robustly reconstructed from two independent varves properties, i.e., the detrital layer thickness (DLT) and grain size ($P99D_0$) respectively, over the 1856-2016 period. The reconstructed Q-mean series suggest that high Q-mean years occurred during the 1925-1960 period and a slight decrease in Q-mean takes place during the second half of the 20th century.
- The same two hydrological parameters of the Naskaupi river, River Q-mean and Q-max, have been also been reconstructed using a rainfall-runoff modeling approach demonstrating the reliability of the two independent reconstruction approaches.
- The statistically significant relation between mean DLT series and the observed Labrador region Q-mean series, extracted from five watersheds of different size and location, demonstrates that Grand Lake varved sequence can also be used as a proxy of regional river discharges conditions.
- The effects of Naskaupi River dyking in 1971 are clearly visible in the sedimentary record and affected sedimentary patterns afterwards. While this event makes the hydroclimatic reconstruction trickier, it remains that the outstanding quality of this varved records provides one of the best hydroclimatic reconstruction from a sedimentary record, with Pearson correlation coefficients up to r = 0.76.

Data availability

The data set used in this study will be available via the information system PANGAEA.

Author contributions

This study is part of AGP's thesis under the supervision of PF and PL. AT and PL provided geophysical data (Fig. 1B, C) and useful information on the morpho-stratigraphical framework of Grand Lake. AGP and DF conducted the coring fieldtrip. AGP and PB collected instrumental data. PB calculated hydro-climatic variables from instrumental data (Fig. 3) and performed the rainfall-runoff modeling. HD and AGP adapted the code used to establish the relationship between the varve parameters and the instrumental data and for the regression model. AGP performed most of the data analysis, wrote the manuscript and created the figures. All authors provided valuable feedback and contributed to the improvement of the manuscript.

Competing interests

The author Pierre Francus is a member of the editorial board of the journal.

Acknowledgments

This research was financially supported by NSERC-Ouranos-Hydro-Québec-Hydro-Manitoba through a CRD grant to P.F. and P.L. (PERSISTANCE project, É. Boucher et al.). This work was also supported by the FRQNT through a doctoral (B2X) research scholarship to A.G.P. and by the MOPGA Short Stay program grant at Université Côte d'Azur, Nice, France to A.G.P and P.B. A financial support for the fieldwork campaign at Grand Lake was provided by POLAR through the NSTP to A.G.P. The authors are grateful to Arnaud De Coninck, David Deligny and Louis-Frédéric Daigle for their participation during fieldwork, laboratory and helpful discussions. We greatly thank Wanda and Dave Blake from North West River for their guiding experience and accommodation at Grand Lake. We thank the Labrador Institute at North West River for the use of their facility during fieldwork. We want to thank Stépahe Ferré from the Micro-Geoarchaeology Laboratory at Université Laval (Québec, QC, Canada) for the production of the high-quality thin sections used in this study. We would also like to thank and Dinis et al., 2019 for sharing a previous version of the R code used for the simple regression model and the X anonymous reviewers for providing constructive comments on this paper. Finally, many thanks to Monique Gagnon and Charles Smith for reviewing the English of an earlier version of the manuscript.

References

Amann, B., Szidat, S., and Grosjean, M.: A millennial-long record of warm season precipitation and flood frequency for the North-western Alps inferred from varved lake sediments: implications for the future, Quaternary. Sci. Rev., 115, 89-100, https://doi.org/10.1016/j.quascirev.2015.03.002, 2015.

Anderson, T.: Rivers of Labrador, Canadian Special Publication of Fisheries and Aquatic Sciences 81, Ottawa, Ontario, 1985.

Appleby, P. and Oldfield, F.: The calculation of lead-210 dates assuming a constant rate of supply of unsupported 210Pb to the sediment, Catena, 5, 1-8, https://doi.org/10.1016/S0341-8162(78)80002-2, 1978.

Bégin, C., Gingras, M., Savard, M. M., Marion, J., Nicault, A., and Bégin, Y.: Assessing tree-ring carbon and oxygen stable isotopes for climate reconstruction in the Canadian northeastern boreal forest, Palaeogeography, Palaeoclimatology, Palaeoecology, 423, 91-101, https://doi.org/10.1016/j.palaeo.2015.01.021, 2015.

Bégin, Y., Nicault, A., Bégin, C., Savard, M. M., Arseneault, D., Berninger, F., Guiot, J., Boreux, J.-J., and Perreault, L.: Analyse dendrochronologique des variations passées du régime hydro climatique au complexe de la grande rivière dans le Nord du Québec, La Houille Blanche, 2007. 70-77, https://doi.org/10.1051/lhb:2007085, 2007.

Bonsal, B.R., Peters, D.L., Seglenieks, F., Rivera, A., and Berg, A.: Changes in freshwater availability across Canada; Chapter 6 in Canada's Changing Climate Report, (ed.) E. Bush and D.S. Lemmen; Government of Canada, Ottawa, Ontario, 2019.

Boucher, E., Nicault, A., Arseneault, D., Bégin, Y., and Karami, M. P.: Decadal Variations in Eastern Canada's Taiga Wood Biomass Production Forced by Ocean-Atmosphere Interactions, Sci. Rep. Uk., 7, 1-13, https://doi.org/10.1038/s41598-017-02580-9, 2017.

Boucher, É., Ouarda, T. B., Bégin, Y., and Nicault, A.: Spring flood reconstruction from continuous and discrete tree ring series, Water. Resour. Res., 47, https://doi.org/10.1029/2010WR010131, 2011.

Briffa, K., Jones, P., Pilcher, J., and Hughes, M.: Reconstructing summer temperatures in northern Fennoscandinavia back to AD 1700 using tree-ring data from Scots pine, Arct. Antartic. Alp. Research., 20, 385-394, https://doi.org/10.1080/00040851.1988.12002691, 1988.

Brigode, P., Brissette, F., Nicault, A., Perreault, L., Kuentz, A., Mathevet, T., and Gailhard, J.: Streamflow variability over the 1881–2011 period in northern Québec: comparison of hydrological reconstructions based on tree rings and geopotential height field reanalysis, Clim. Past, 12, 1785-1804, https://doi.org/10.5194/cp-12-1785-2016, 2016.

Cherry, J. E., Knapp, C., Trainor, S., Ray, A. J., Tedesche, M., and Walker, S.: Planning for climate change impacts on hydropower in the Far North, Hydrol. Earth Syst. Sci., 21, 133, https://doi:10.5194/hess-21-133-2017, 2017.

Cockburn, J. M. and Lamoureux, S. F.: Inflow and lake controls on short-term mass accumulation and sedimentary particle size in a High Arctic lake: implications for interpreting varved lacustrine sedimentary records, J. Paleolimnol., 40, 923-942, https://doi.org/10.1007/s10933-008-9207-5, 2008.

Collins, M., Knutti, R., Arblaster, J., Dufresne, J-L., Fichefet, T., Friedlingstein, P., Gao, X., Gutowski, W. J., Johns, T., Krinner, G., Shongwe, M., Tebaldi, C., Weaver, A. J., Wehner, M. F., Allen, M. R., Andrews, T., Beyerle, U., Bitz, C. M., Bony, S., & Booth, B. B. B.: Long-term climate change: projections, commitments and irreversibility, In: Climate Change 2013 - The Physical Science Basis, Contribution of Working Group I to the Fifth Assessment Report of the Intergovernmental Panel on Climate Change, Intergovernmental Panel on Climate Change, Cambridge University Press, 1029-1136, 2013.

Compo, G. P., Whitaker, J. S., Sardeshmukh, P. D., Matsui, N., Allan, R. J., Yin, X., Gleason, B. E., Vose, R. S., Rutledge, G., and Bessemoulin, P.: The twentieth century reanalysis project, Q J R Meteorol Soc, 137, 1-28, https://doi.org/10.1002/qj.776, 2011.

Cook, E. R., Meko, D. M., Stahle, D. W., and Cleaveland, M. K.: Drought reconstructions for the continental United States, J. Clim., 12, 1145-1162, https://doi.org/10.1175/1520-0442(1999)012%3C1145:DRFTCU%3E2.0.CO;2, 1999.

Coron, L., Thirel, G., Delaigue, O., Perrin, C., and Andréassian, V.: The suite of lumped GR hydrological models in an R package, Environmental Modelling & Software, 94, 166-171, https://doi.org/10.1016/j.envsoft.2017.05.002, 2017.

Croudace, I. W., Rindby, A., and Rothwell, R. G.: ITRAX: description and evaluation of a new multi-function X-ray core scanner, Geological Society, London, Special Publications, 267, 51-63, https://doi.org/10.1144/GSL.SP.2006.267.01.04, 2006.

Cuven, S., Francus, P., and Lamoureux, S.: Mid to Late Holocene hydroclimatic and geochemical records from the varved sediments of East Lake, Cape Bounty, Canadian High

https://doi.org/10.5194/cp-2020-87
Preprint. Discussion started: 20 July 2020

Arctic, Quaternary. Sci. Rev., 30, 2651-2665, https://doi.org/10.1016/j.quascirev.2011.05.019, 2011.

Cuven, S., Francus, P., and Lamoureux, S. F.: Estimation of grain size variability with micro X-ray fluorescence in laminated lacustrine sediments, Cape Bounty, Canadian High Arctic, J. Paleolimnol., 44, 803-817, https://doi.org/10.1007/s10933-010-9453-1, 2010.

Czymzik, M., Dulski, P., Plessen, B., Von Grafenstein, U., Naumann, R., and Brauer, A.: A 450 year record of spring-summer flood layers in annually laminated sediments from Lake Ammersee (southern Germany), Water. Resour. Res., 46, https://doi.org/10.1029/2009WR008360, 2010.

Czymzik, M., Haltia, E., Saarni, S., Saarinen, T., and Brauer, A.: Differential North Atlantic control of winter hydroclimate in late Holocene varved sediments of Lake Kortejärvi, eastern Finland, Boreas, 47, 926-937, https://doi.org/10.1111/bor.12315, 2018.

D'Arrigo, R., Buckley, B., Kaplan, S., and Woollett, J.: Interannual to multidecadal modes of Labrador climate variability inferred from tree rings, Clim. Dynam., 20, 219-228, https://doi.org/10.1007/s00382-002-0275-3, 2003.

Déry, S. J. and Wood, E. F.: Decreasing river discharge in northern Canada, Geophys. Res. Lett., 32, https://doi.org/10.1029/2005GL022845, 2005.

Dinis, L., Bégin, C., Savard, M. M., Marion, J., Brigode, P., and Alvarez, C.: Tree-ring stable isotopes for regional discharge reconstruction in eastern Labrador and teleconnection with the Arctic Oscillation, Clim. Dynam., 53, 3625-3640, https://doi.org/10.1007/s00382-019-04731-2, 2019.

Fitzhugh, W.: Environmental Approaches to the Prehistory of the North, Journal of the Washington Academy of Sciences, 1973. 39-53, 1973.

Francus, P.: An image-analysis technique to measure grain-size variation in thin sections of soft clastic sediments, Sedimentary Geology, 121, 289-298, https://doi.org/10.1016/S0037-0738(98)00078-5, 1998.

Francus, P., Bradley, R. S., Abbott, M. B., Patridge, W., and Keimig, F.: Paleoclimate studies of minerogenic sediments using annually resolved textural parameters, Geophys. Res. Lett., 29, 59-51-59-54, https://doi.org/10.1029/2002GL015082, 2002.

Francus, P. and Cosby, C. A.: Sub-sampling unconsolidated sediments: A solution for the preparation of undistrubed thin-sections from clay-rich sediments, J. Paleolimnol, 26, 323-326, https://doi.org/10.1023/A:1017572602692, 2001.

Francus, P. and Karabanov, E.: A computer-assisted thin-section study of Lake Baikal sediments: a tool for understanding sedimentary processes and deciphering their climatic signal, Int. J. Earth. Sci., 89, 260-267, https://doi.org/10.1007/s005319900064, 2000.

Francus, P. and Nobert, P.: An integrated computer system to acquire, process, measure and store images of laminated sediments, In 4th International limnogeology congress, Barcelona, July, 2007.

Fulton, R. J. and Ferguson, J.: Surficial Geology Cartwright: Labrador, Newfoundland, Commission, Department of Energy, Mines and Resources, 1986.

Gilbert, R. and Desloges, J. R.: Late glacial and Holocene sedimentary environments of Quesnel Lake, British Columbia, Geomorphology, 179, 186-196, https://doi.org/10.1016/j.geomorph.2012.08.010, 2012.

Gupta, H. V., Kling, H., Yilmaz, K. K., and Martinez, G. F.: Decomposition of the mean squared error and NSE performance criteria: Implications for improving hydrological modelling, J. Hydrol., 377, 80-91, https://doi.org/10.1016/j.jhydrol.2009.08.003, 2009.

Hardy, D. R., Bradley, R. S., and Zolitschka, B.: The climatic signal in varved sediments from Lake C2, northern Ellesmere Island, Canada, J. Paleolimnol., 16, 227-238, https://doi.org/10.1007/BF00176938, 1996.

Heideman, M., Menounos, B., and Clague, J. J.: An 825-year long varve record from Lillooet Lake, British Columbia, and its potential as a flood proxy, Quaternary. Sci. Rev., 126, 158-174, https://doi.org/10.1016/j.quascirev.2015.08.017, 2015.

Jandhyala, V. K., Liu, P., and Fotopoulos, S. B.: River stream flows in the northern Québec Labrador region: A multivariate change point analysis via maximum likelihood, Water. Resour. Res., 45, https://doi.org/10.1029/2007WR006499, 2009.

Kaufman, C. A., Lamoureux, S. F., and Kaufman, D. S.: Long-term river discharge and multidecadal climate variability inferred from varved sediments, southwest Alaska, Quat. Res., 76, 1-9, https://doi.org/10.1016/j.yqres.2011.04.005, 2011.

Kuentz, A., Mathevet, T., Gailhard, J., and Hingray, B.: Building long-term and high spatio-temporal resolution precipitation and air temperature reanalyses by mixing local observations and global atmospheric reanalyses: the ANATEM model, Hydrol. Earth Syst. Sci., 19, 2717-2736, https://doi.org/10.5194/hess-19-2717-2015, 2015.

Kylander, M. E., Ampel, L., Wohlfarth, B., and Veres, D.: High-resolution X-ray fluorescence core scanning analysis of Les Echets (France) sedimentary sequence: new insights from chemical proxies, J. Quat. Sci., 26, 109-117, https://doi.org/10.1002/jqs.1438, 2011.

Lamoureux, S.: Five centuries of interannual sediment yield and rainfall-induced erosion in the Canadian High Arctic recorded in lacustrine varves, Water. Resour. Res., 36, 309-318, https://doi.org/10.1029/1999WR900271, 2000.

Lamoureux, S. F.: Embedding unfrozen lake sediments for thin section preparation, J. Paleolimnol., 10, 141-146, https://doi.org/10.1007/BF00682510, 1994.

Lamoureux, S. F., Stewart, K. A., Forbes, A. C., and Fortin, D.: Multidecadal variations and decline in spring discharge in the Canadian middle Arctic since 1550 AD, Geophys. Res. Lett., 33, https://doi.org/10.1029/2005GL024942, 2006.

Lapointe, F., Francus, P., Lamoureux, S. F., Saïd, M., and Cuven, S.: 1750 years of large rainfall events inferred from particle size at East Lake, Cape Bounty, Melville Island, Canada, J. paleolimnol., 48, 159-173, https://doi.org/10.1007/s10933-012-9611-8, 2012.

Linderholm, H. W., Nicolle, M., Francus, P., Gajewski, K., Helama, S., Korhola, A., Solomina, O., Yu, Z., Zhang, P., D'Andrea, W. J., Debret, M., Divine, D. V., Gunnarson, B. E., Loader, N. J., Massei, N., Seftigen, K., Thomas, E. K., Werner, J., Andersson, S., Berntsson, A., Luoto, T. P., Nevalainen, L., Saarni, S., and Väliranta, M.: Arctic hydroclimate variability during the last 2000 years: current understanding and research challenges, Clim. Past, 14, 473–514, https://doi.org/10.5194/cp-14-473-2018, 2018.

Ljungqvist, F. C., Krusic, P. J., Sundqvist, H. S., Zorita, E., Brattström, G., and Frank, D.: Northern Hemisphere hydroclimate variability over the past twelve centuries, Nature, 532, 94-98, https://doi.org/10.1038/nature17418, 2016.

Mangili, C., Brauer, A., Moscariello, A., and Naumann, R.: Microfacies of detrital event layers deposited in Quaternary varved lake sediments of the Piànico-Sèllere Basin (northern Italy), Sedimentology, 52, 927-943, https://doi.org/10.1111/j.1365-3091.2005.00717.x, 2005.

Mortsch, L., Cohen, S., and Koshida, G.: Climate and water availability indicators in Canada: Challenges and a way forward. Part II–Historic trends, Can. Water Resour. J., 40, 146-159, https://doi.org/10.1080/07011784.2015.1006024, 2015.

Naulier, M., Savard, M. M., Bégin, C., Gennaretti, F., Marion, J., Nicault, A., and Bégin, Y.: A millennial summer temperature reconstruction for northeastern Canada using oxygen isotopes in subfossil trees, Clim. Past, 11, 1153-1164, https://doi.org/10.5194/cp-11-1153-2015, 2015.

Naulier, M., Savard, M. M., Bégin, C., Marion, J., Arseneault, D., and Bégin, Y.: Carbon and oxygen isotopes of lakeshore black spruce trees in northeastern Canada as proxies for climatic reconstruction, Chem. Geol., 374, 37-43, https://doi.org/10.1016/j.chemgeo.2014.02.031, 2014.

Nicault, A., Boucher, E., Bégin, C., Guiot, J., Marion, J., Perreault, L., Roy, R., Savard, M. M., and Bégin, Y.: Hydrological reconstruction from tree-ring multi-proxies over the last two centuries at the Caniapiscau Reservoir, northern Québec, Canada, J. Hydrol., 513, 435-445, https://doi.org/10.1016/j.jhydrol.2014.03.054, 2014.

Normandeau, A., Lajeunesse, P., Poiré, A. G., and Francus, P.: Morphological expression of bedforms formed by supercritical sediment density flows on four fjord-lake deltas of the south-eastern Canadian Shield (Eastern Canada), Sedimentology, 63, 2106-2129, https://doi.org/10.1111/sed.12298, 2016.

Notzl, L., Greene, R., and Riley, J.: Labrador Nature Atlas. Vol. II. Ecozones, Ecoregions, and Ecodistricts, Nature Conservancy of Canada and Province of Newfoundland and Labrador, Toronto, ON, Canada, 2013.

Ojala, A. E. and Alenius, T.: 10 000 years of interannual sedimentation recorded in the Lake Nautajärvi (Finland) clastic–organic varves, Palaeogeography, Palaeoclimatology, Palaeoecology, 219, 285-302, https://doi.org/10.1016/j.palaeo.2005.01.002, 2005.

Ojala, A. E., Kosonen, E., Weckström, J., Korkonen, S., and Korhola, A.: Seasonal formation of clastic-biogenic varves: the potential for palaeoenvironmental interpretations, GFF, 135, 237-247, https://doi.org/10.1080/11035897.2013.801925, 2013.

Oudin, L., Hervieu, F., Michel, C., Perrin, C., Andréassian, V., Anctil, F., and Loumagne, C.: Which potential evapotranspiration input for a lumped rainfall–runoff model?: Part 2—Towards a simple and efficient potential evapotranspiration model for rainfall–runoff modelling, J. Hydrol., 303, 290-306, https://doi.org/10.1016/j.jhydrol.2004.08.026, 2005.

Perrin, C., Michel, C., and Andréassian, V.: Improvement of a parsimonious model for streamflow simulation, J. Hydrol., 279, 275-289, https://doi.org/10.1016/S0022-1694(03)00225-7, 2003.

Rohde, R., Muller, R., Jacobsen, R., Muller, E., Perlmutter, S., Rosenfeld, A., Wurtele, J., Groom, D., and Wickham, C.: A New Estimate of the Average Earth Surface Land Temperature Spanning 1753 to 2011, Geoinfor. Geostat.: An Overview 1: 1, of, 7, 2, http://dx.doi.org/10.4172/2327-4581.1000101, 2013.

Saarni, S., Lensu, A., Tammelin, M., Haltia, E., and Saarinen, T.: Winter climate signal in boreal clastic-biogenic varves: a comprehensive analysis of three varved records from 1890 to 1990 AD with meteorological and hydrological data from Eastern Finland, GFF, 139, 314-326, https://doi.org/10.1080/11035897.2017.1389984, 2017.

Saarni, S., Saarinen, T., and Dulski, P.: Between the North Atlantic Oscillation and the Siberian High: A 4000-year snow accumulation history inferred from varved lake sediments in Finland, Holocene, 26, 423-431, https://doi.org/10.1177/0959683615609747, 2016.

Schillereff, D. N., Chiverrell, R. C., Macdonald, N., and Hooke, J. M.: Flood stratigraphies in lake sediments: A review, Earth-Sci. Rev., 135, 17-37, https://doi.org/10.1016/j.earscirev.2014.03.011, 2014.

Seiller, G., Anctil, F., and Perrin, C.: Multimodel evaluation of twenty lumped hydrological models under contrasted climate conditions, Hydrol. Earth Syst. Sci., https://dx.doi.org/10.5194/hess-1116-1171-2012, 2012.

Snowball, I., Sandgren, P., and Petterson, G.: The mineral magnetic properties of an annually laminated Holocene lake-sediment sequence in northern Sweden, Holocene, 9, 353-362, https://doi.org/10.1191/095968399670520633, 1999.

St-Onge, G., Mulder, T., Francus, P., and Long, B.: Chapter two continuous physical properties of cored marine sediments, Developments in marine geology, 1, 63-98, https://doi.org/10.1016/S1572-5480(07)01007-X, 2007.

Stocker, T. F., Qin, D., Plattner, G.-K., Tignor, M. M., Allen, S. K., Boschung, J., Nauels, A., Xia, Y., Bex, V., and Midgley, P. M.: Climate change 2013: the physical science basis. Contribution of working group I to the fifth assessment report of IPCC the

https://doi.org/10.5194/cp-2020-87
Preprint. Discussion started: 20 July 2020

intergovernmental panel on climate change. Cambridge University Press, https://dx.doi.org/10.1017/CBO9781107415324, 2014.

Sveinsson, O. G., Lall, U., Fortin, V., Perrault, L., Gaudet, J., Zebiak, S., and Kushnir, Y.: Forecasting spring reservoir inflows in Churchill Falls basin in Quebec, Canada, J. Hydrol. Eng., 13, 426-437, https://dx.doi.org/10.1061/(Asce)1084-0699(2008)13:6(426), 2008.

R Core Team: R: A Language and Environment for Statistical Computing, R Foundation for Statistical Computing, Vienna, Austria, http://www.R-project.org/, 2019.

Tomkins, J. D., Lamoureux, S. F., Antoniades, D., and Vincent, W. F.: Autumn snowfall and hydroclimatic variability during the past millennium inferred from the varved sediments of meromictic Lake A, northern Ellesmere Island, Canada, Quat. Res., 74, 188-198, https://doi.org/10.1016/j.yqres.2010.06.005, 2010.

Trottier, A. P., Lajeunesse, P., Gagnon-Poiré, A., and Francus, P.: Morphological signatures of deglaciation and postglacial sedimentary processes in a deep fjord-lake (Grand Lake, Labrador), Earth Surf. Proc. Land., 45, 928-947, https://doi.org/10.1002/esp.4786, 2020.

Valéry, A., Andréassian, V., and Perrin, C.: 'As simple as possible but not simpler': What is useful in a temperature-based snow-accounting routine? Part 1–Comparison of six snow accounting routines on 380 catchments, J. Hydrol, 517, 1166-1175, https://doi.org/10.1016/j.jhydrol.2014.04.059, 2014a.

Valéry, A., Andréassian, V., and Perrin, C.: 'As simple as possible but not simpler': What is useful in a temperature-based snow-accounting routine? Part 2–Sensitivity analysis of the Cemaneige snow accounting routine on 380 catchments, J. Hydrol., 517, 1176-1187, https://doi.org/10.1016/j.jhydrol.2014.04.058, 2014b.

Viau, A. E. and Gajewski, K.: Reconstructing millennial-scale, regional paleoclimates of boreal Canada during the Holocene, J. Clim., 22, 316-330, https://doi.org/10.1175/2008JCLI2342.1, 2009.

Zhang, X., Harvey, K. D., Hogg, W., and Yuzyk, T. R.: Trends in Canadian streamflow, Water Resour. Res., 37, 987-998, https://doi.org/10.1029/2000WR900357, 2001.

Zolitschka, B., Francus, P., Ojala, A. E., and Schimmelmann, A.: Varves in lake sediments–a review, Quaternary. Sci. Rev., 117, 1-41, https://doi.org/10.1016/j.quascirev.2015.03.019, 2015.